Improved Regional Geoid in the Weddell Sea Region, Antarctica, from Heterogeneous Terrestrial Gravity Data

– Electronic supplementary material –

Joachim Schwabe and Mirko Scheinert

Mirko Scheinert
Institut für Planetare Geodäsie
Technische Universität Dresden
01062 Dresden
Germany

E-mail: mirko.scheinert@tu-dresden.de
Phone: +49(0)351-463-33683
Fax: +49(0)351-463-37063

1 Description of data grid

Table 1: Format description of ASCII grid file and meta information.
Grid domain: 70°W–0°W, 82°S–62°S, spacing 0.125° (7.5') by 0.041667° (2.5')
Order of records: One record per line in scanline format (west to east, north to south)

column	quantity	unit	tide system	reference ellipsoid
1	longitude	degrees	not applicable	WGS84
2	latitude	degrees	not applicable	WGS84
3	height anomaly	m	tide-free	WGS84
4	geoid	m	mean-tide	Topex
5	geoid–quasigeoid separation	m	not applicable	not applicable
6	estimated uncertainty	m	not applicable	not applicable
7	estimated empirical resolution	km	not applicable	not applicable

2 Supplementary figures and tables

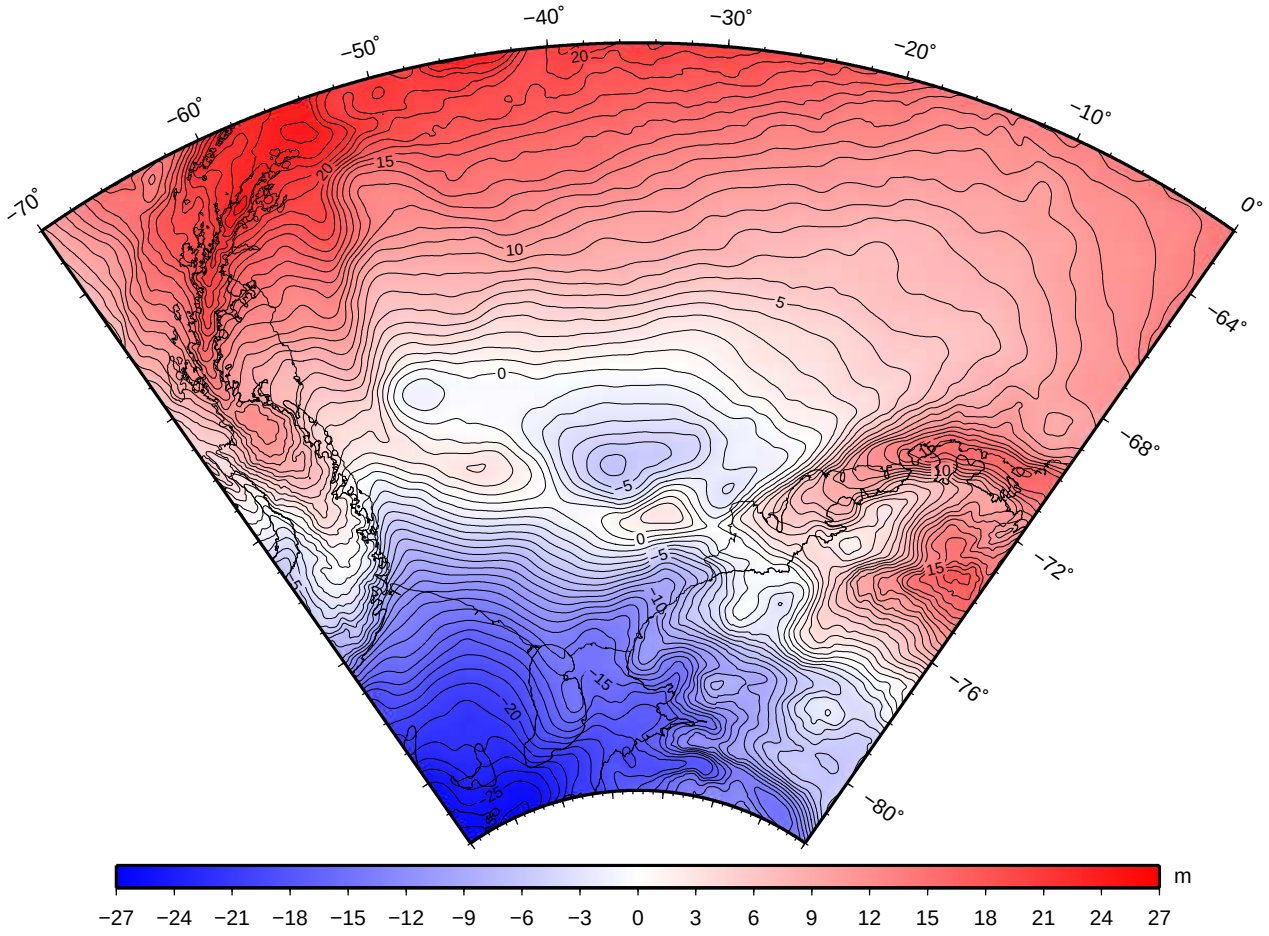

Figure 1: Improved geoid in the mean-tide system w.r.t. the Topex ellipsoid (data column 4 in Table 1)

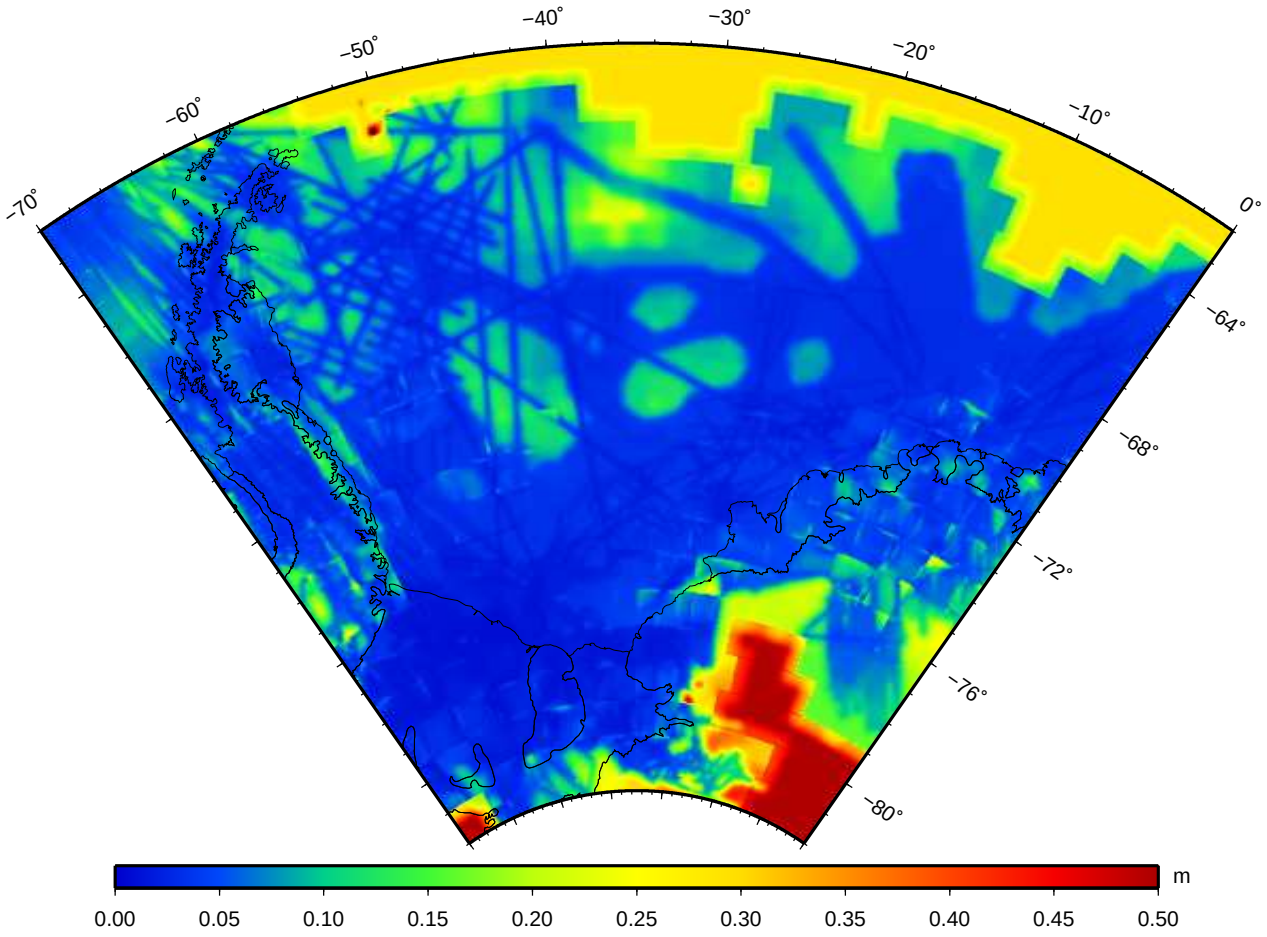

Figure 2: Over-all uncertainty of the improved geoid (Fig. 1) as a combination of LSC error estimates and the r.m.s. misfit of the averaged tiles, whichever is larger (data column 6 in Table 1)

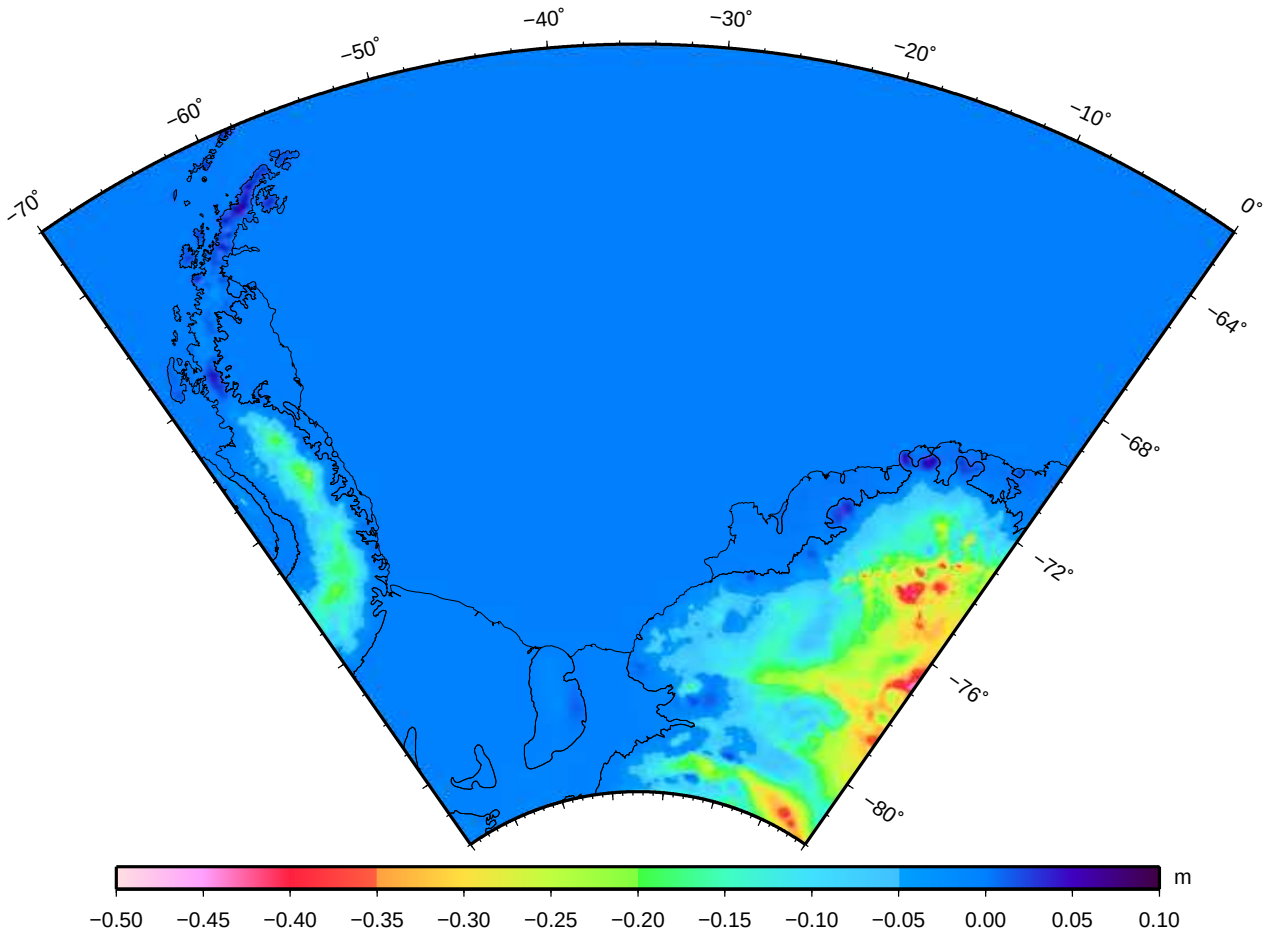

Figure 3: Estimated geoid–quasigeoid separation (data column 5 in Table 1)

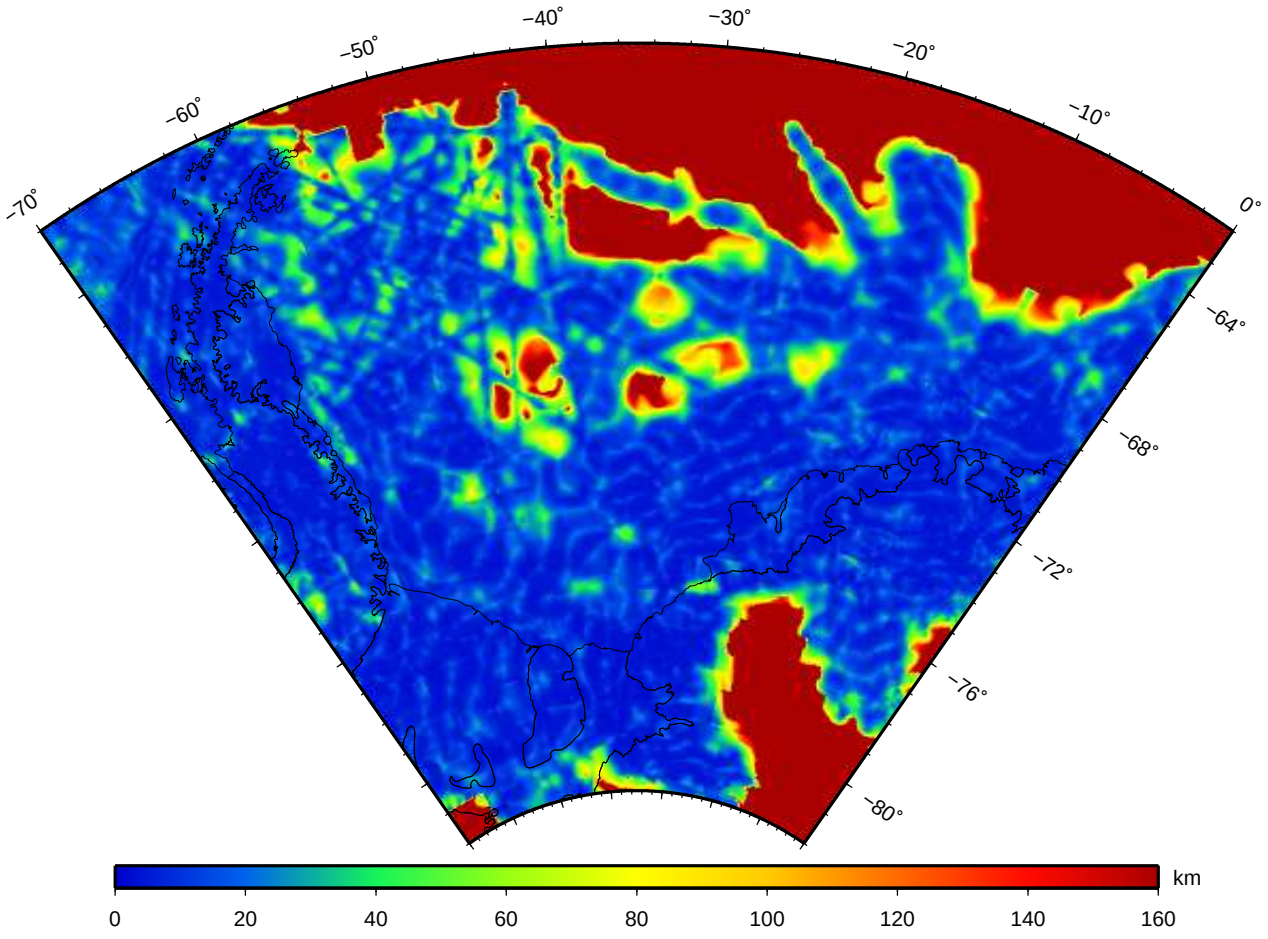

Figure 4: Empirically estimated resolution of the residual geoid as defined by the radius where the accumulated r.m.s. of the signal attains the over-all uncertainty (data column 7 in Table 1)

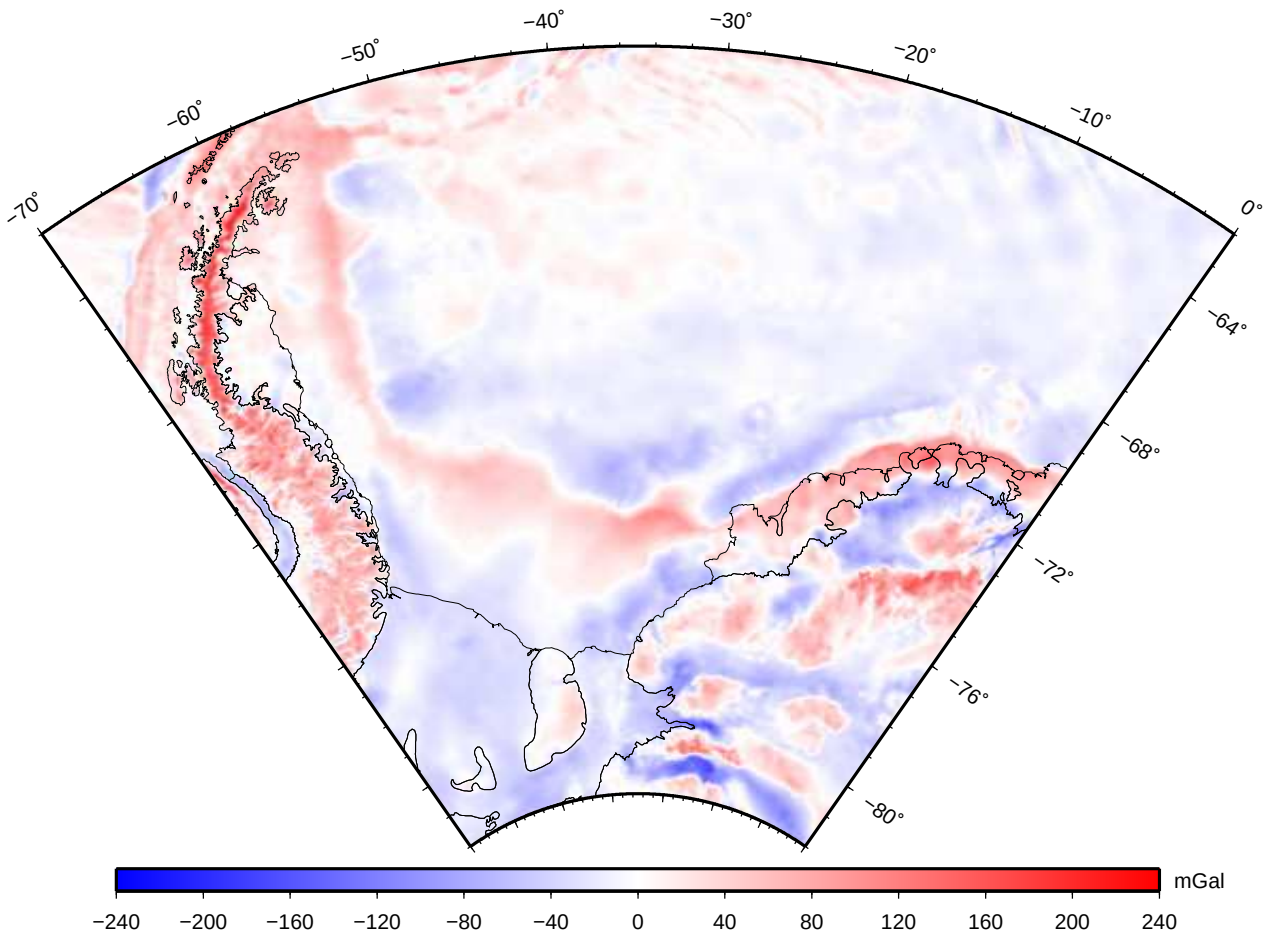

Figure 5: Improved free-air gravity anomaly at surface altitude

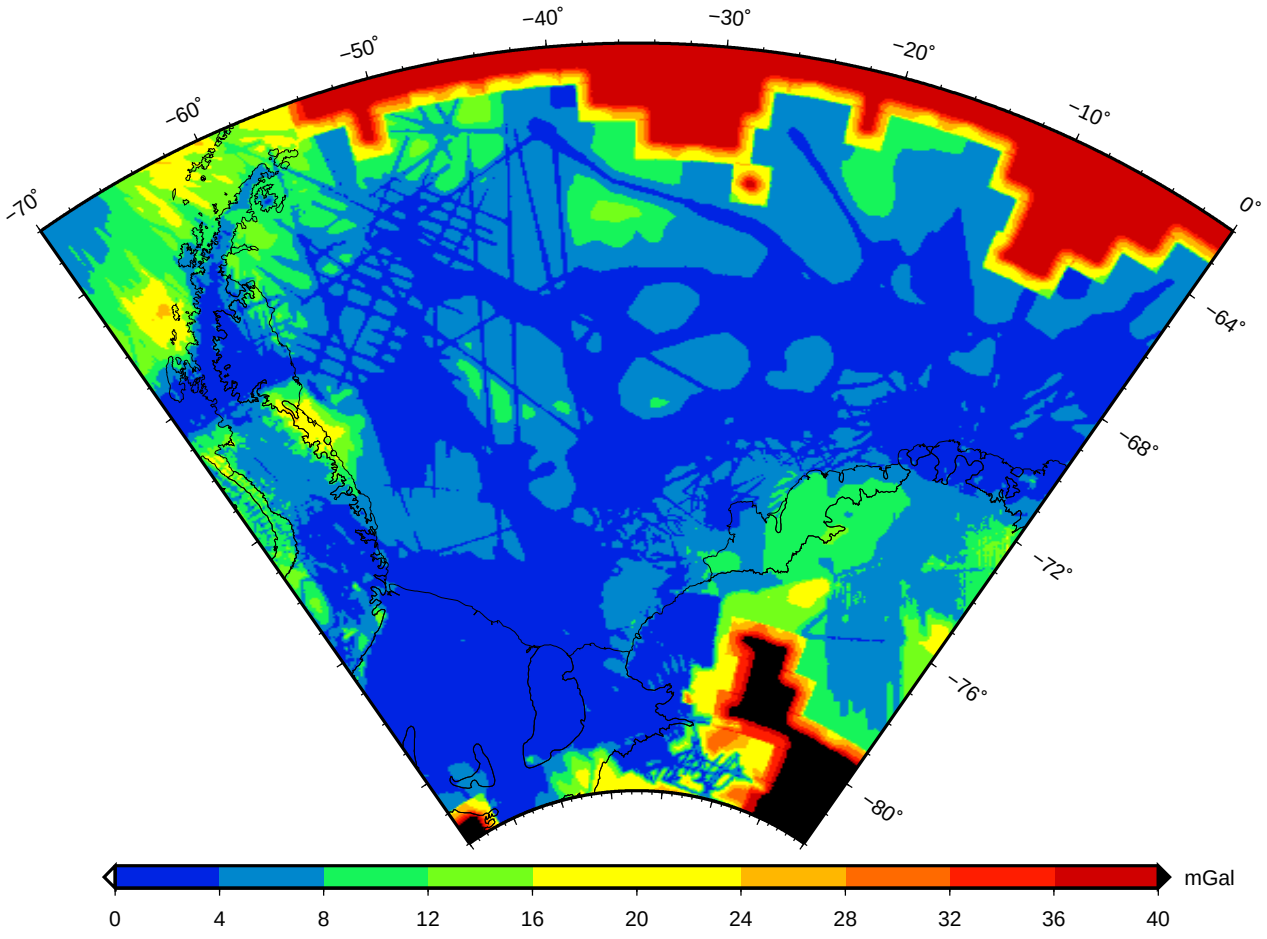

Figure 6: Over-all uncertainty of the improved gravity anomaly (Fig. 4) as a combination of LSC error estimates and the r.m.s. misfit of the averaged tiles, whichever is larger

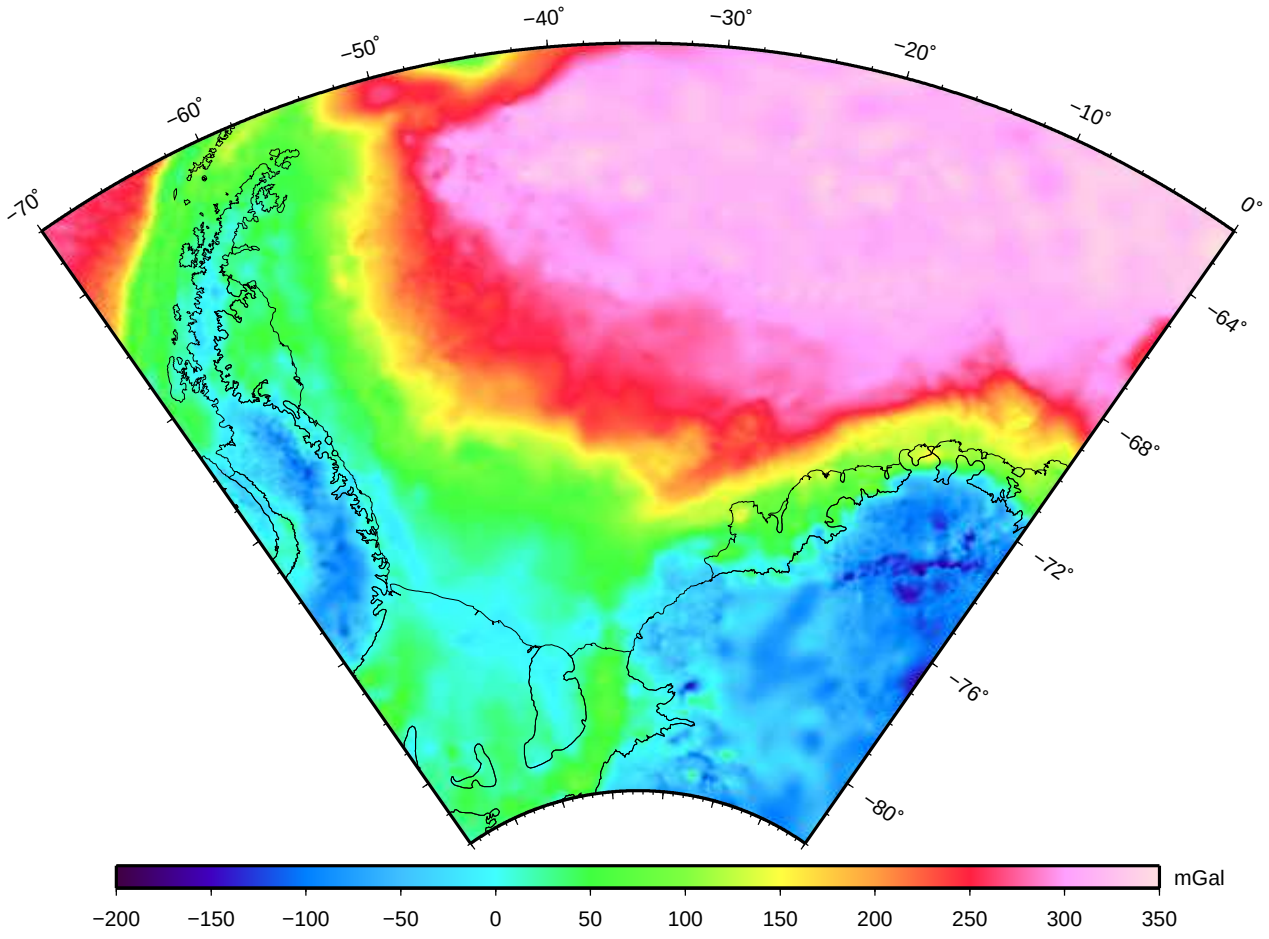

Figure 7: Complete Bouguer anomaly, based on the full topographic effect of the BEDMAP2 ice surface topography, bedrock topography, and bathymetry

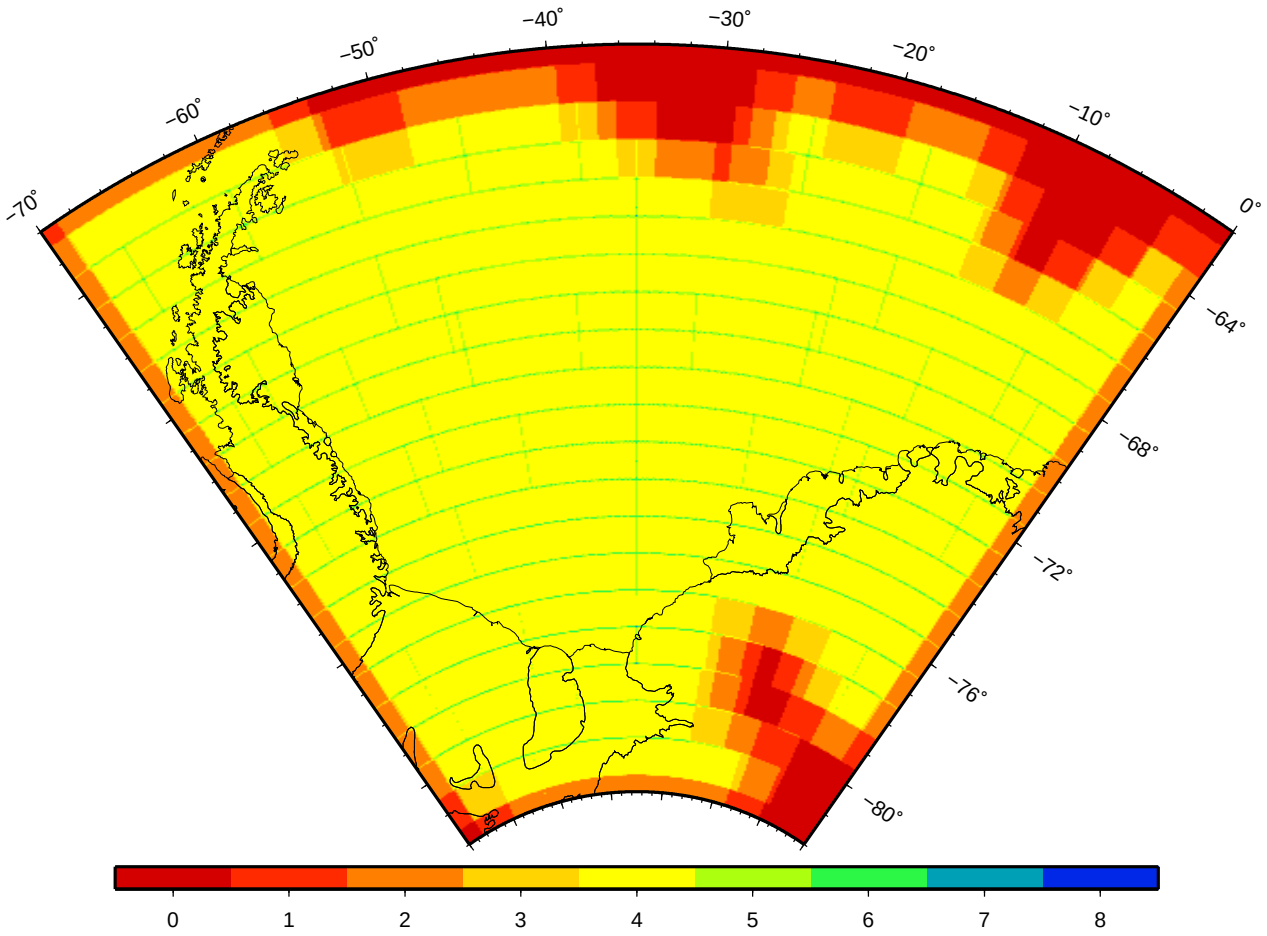

Figure 8: Number of overlapping tiles contributing to each grid node

Table 2: A-posteriori cross-over differences at altitude corrected for estimated profile biases. Numbers in italics refer to isostatic anomalies. In case of internal cross-overs signs of differences were associated with the respective sign of the height difference by convention

datasets	land and ice shelf areas							ocean areas						
	mean		SD		max		no.	mean		SD		max		no.
internal cross-overs														
ADGRAV								+0.0	*+0.0*	2.3	*2.3*	11	*11*	1222
BAS-1996	–2.2	*–2.2*	3.6	*3.6*	6	*6*	3							
BAS-Evans	–4.6	*–4.6*	8.6	*8.6*	9	*9*	4							
BAS-JRI	–1.6	*–1.0*	4.9	*4.9*	11	*11*	25	+0.2	*0.0*	5.5	*5.6*	18	*17*	94
BAS-SPARC	+1.1	*+1.1*	8.1	*8.1*	11	*11*	6							
IceBridge	+4.0	*+0.9*	18.4	*6.1*	87	*33*	947	+0.1	*0.0*	2.6	*2.5*	23	*19*	2925
USAC								–0.1	*–0.1*	0.6	*0.6*	4	*4*	87
VISA	1.2	*1.2*	8.3	*8.3*	28	*28*	257							
external cross-overs														
IceBridge – ADGRAV								+1.6	*+1.2*	3.4	*3.3*	12	*12*	418
IceBridge – BAS-1996	–12.5	*+0.4*	24.9	*13.1*	108	*78*	280	+14.3	*+6.4*	20.3	*12.7*	52	*36*	12
IceBridge – BAS-Evans	–7.6	*–1.2*	14.5	*5.6*	30	*10*	12							
IceBridge – BAS-JRI	–4.7	*+1.7*	21.6	*19.9*	96	*82*	43	+5.8	*+3.6*	8.5	*7.9*	30	*22*	78
IceBridge – BAS-SPARC	–1.2	*+1.0*	16.8	*11.5*	70	*76*	646							
IceBridge – USAC								+0.8	*+0.7*	6.1	*6.1*	25	*25*	192
ADGRAV – USAC								+2.5	*+2.5*	6.0	*6.0*	12	*12*	17
ADGRAV – VISA								+7.0	*+2.8*	11.4	*9.3*	28	*23*	53
BAS-1996 – BAS-SPARC	–1.5	*–1.5*	6.8	*6.8*	12	*12*	8							